Fusion Pore Conductance: Experimental Approaches and Theoretical Algorithms

Vladimir Ratinov, Ilya Plonsky, and Joshua Zimmerberg
Laboratory of Cellular and Molecular Biophysics, National Institute of Child Health and Human Development, National Institutes of Health, Bethesda, Maryland 20892-1855 USA

ABSTRACT Time-resolved admittance measurements provide the basis for studies showing that membrane fusion occurs through the formation and widening of an initially small pore, linking two previously separated aqueous compartments. Here we introduce modifications to this method that correct the cell-pipette (source) admittance for attenuation and phase shifts produced by electrophysiological equipment. Two new approaches for setting the right phase angle are discussed. The first uses the displacement of a patch-clamp amplifier C-slow potentiometer for the calculation of phase. This calculation is based on amplitudes of observed and expected (theoretical) changes in the source admittance. The second approach automates the original phase adjustment, the validity of which we prove analytically for certain conditions. The multiple sine wave approach is modified to allow the calculation of target cell membrane parameters and the conductance of the fusion pore. We also show how this technique can be extended for measurements of the resting potential of the first (voltage-clamped) membrane. We introduce an algorithm for calculation of fusion pore conductance despite a concurrent change in the resistance of the clamped membrane. The sensitivity of the capacitance restoration algorithm to phase shift errors is analyzed, and experimental data are used to demonstrate the results of this analysis. Finally, we show how the phase offset can be corrected "off-line" by restoring the shape of the capacitance increment.

GLOSSARY

a	Real part of Q
A_2	Real part of Y_2
$A_2(\omega_k)$	Values of A_2 for two-sine-wave stimulus in MSW ($k = 1, 2$)
A_{err}	Real part of $(Y_2)_{out}$
A_{in}	Real part of the signal at the input of PSD
A_{out}	Real part of Y_{out}
A_t	Real part of Y_t
A_{tbf}	Real part of Y_{tbf}
$A_{tbf}(\omega_1)$	Real part of Y_{tbf} for the first sine wave stimulus in MSW
$A_{tbf}(\omega_2)$	Real part of Y_{tbf} for the second sine wave stimulus in MSW
$A_{tbf}(\omega_k)$	Values of the real part of Y_{tbf} for two-sine-wave stimulus in MSW ($k = 1, 2$)
b	Imaginary part of Q
B_2	Imaginary part of Y_2
$B_2(\omega_k)$	Values of B_2 for two sine-wave-stimulus in MSW ($k = 1, 2$)
B_{err}	Imaginary part of $(Y_2)_{out}$
B_{in}	Imaginary part of the signal at the input of PSD
B_{out}	Imaginary part of Y_{out}
B_t	Imaginary part of Y_t
B_{tbf}	Imaginary part of Y_{tbf}
$B_{tbf}(\omega_1)$	Imaginary part of Y_{tbf} for the first sine wave stimulus in MSW
$B_{tbf}(\omega_2)$	Imaginary part of Y_{tbf} for the second sine wave stimulus in MSW
$B_{tbf}(\omega_k)$	Values of the imaginary part of Y_{tbf} for two-sine-wave stimulus in MSW ($k = 1, 2$)
c_1	Real part of Y_1 for the first sine wave stimulus in MSW
c_2	Real part of Y_1 for the second sine wave stimulus in MSW
c_k	Real parts of $Y_1(\omega_k)$ ($k = 1, 2$)
C_{err}	Error in the calculated value of C_{m2} due to the phase offset
C_{m1}	Capacitance of the first (initially clamped) membrane
ΔC_{m1}	Change in C_{m1}
C_{m2}	Capacitance of the second (initially nonclamped) membrane
C_{sl}	C-slow potentiometer in the capacitance neutralization circuitry of a patch-clamp amplifier
ΔC_{sl}	Increment of C-slow potentiometer of a patch-clamp amplifier
d_1	Imaginary part of Y_1 for the first sine wave stimulus in MSW
d_2	Imaginary part of Y_1 for the second sine wave stimulus in MSW
d_k	Imaginary parts of $Y_1(\omega_k)$ ($k = 1, 2$)
E_r	Resting potential of the first (initially clamped) membrane
f	Frequency of the stimulating sine wave
g_1	B_2 value for the first sine wave stimulus in modified MSW
g_2	B_2 value for the second sine wave stimulus in modified MSW

Received for publication 3 March 1997 and in final form 28 January 1998.

Address reprint requests to Dr. Joshua Zimmerberg, National Institutes of Health, Bldg. 10, Rm. 10D14, 10 Center Dr., MSC 1855, Bethesda, MD 20892-1855. Tel.: 301-496-6571; Fax: 301-594-0813; E-mail: joshz@helix.nih.gov.

0006-3495/98/05/2374/14 $2.00

g_k Same as $A_2(\omega_k)$ ($k = 1, 2$)
$G1_{m1}$ Changed value of G_{m1}
G_a Access (pipette) conductance
G_{DC} Direct current conductance
G_{err} Error in the calculated value of G_p due to the phase offset
G_{m1} Conductance of the first (initially clamped) membrane
ΔG_{m1} Increment of G_{m1}
G_{m2} Conductance of the second (initially nonclamped) membrane
G_p Conductance of the fusion pore
G_{sr} G-series potentiometer in the capacitance neutralization circuitry of a patch-clamp amplifier
h_1 A_2 value for the first sine wave stimulus in modified MSW
h_2 A_2 value for the second sine wave stimulus in modified MSW
h_k Same as $B_2(\omega_k)$
I Imaginary part of $(Y_{incr})_{out}$
I_h Holding current
I_k Imaginary parts of $[Y_{incr}(\omega_k)]_{out}$
J Increment of Y_t during the C-slow jump
J_{out} J as measured from the output of PSD
$J1_{out}$ J_{out} when phase deviates from φ_{NM}
K Factor that represents attenuation of Y_t caused by equipment
Q Ratio of J and J_{out}
R Real part of $(Y_{incr})_{out}$
R_a Access (pipette) resistance
R_k Real parts of $[Y_{incr}(\omega_k)]_{out}$ ($k = 1, 2$)
R_{m1} Resistance of the first (initially clamped) membrane
R_{m2} Resistance of the second (initially nonclamped) membrane
R_p Fusion pore resistance
$T(\omega)$ Scaling factor as defined in Eq. 21
$T(\omega_k)$ Values of $T(\omega)$ for both sine wave stimuli in modified MSW ($k = 1, 2$)
U_h Holding potential
Y_1 Admittance of R_a and Y_{m1} in series
$Y_1(\omega_k)$ Values of Y_1 for two-sine-wave stimulus in MSW ($k = 1, 2$)
$Y1_{comp}$ Admittance of the compensation circuitry after a C-slow jump is issued
$Y1_t$ Total admittance after a C-slow jump is issued
Y_2 Admittance of G_p and Y_{m2} in series
$(Y_2)_{out}$ Value of Y_2 measured at the output of PSD
$Y_2(\omega_k)$ Values of Y_2 for two-sine-wave stimulus in MSW ($k = 1, 2$)
Y_3 Admittance of R_a and Y_{m1+2} in series
Y_{comp} Admittance of the capacitance neutralization circuitry
Y_G Sum of Y_2 and ΔG_{m1}
Y_{in} Signal at the input of the PSD
Y_{incr} Fusion-induced increment of the total admittance, Y_t
$(Y_{incr})_{out}$ Y_{incr}, as recorded from the output of PSD
$[Y_{incr}(\omega_k)]_{out}$ Values of $(Y_{incr})_{out}$ for both sine wave stimuli in modified MSW
Y_{m1} Admittance of the first (initially clamped) membrane
Y_{m1+2} Admittance of Y_{m1} and Y_2 in parallel
Y_{m2} Admittance of the second (initially nonclamped) membrane
Y_{out} Signal from the output of PSD
$\Delta Y_{out}(\varphi)$ ΔC_{m1}-induced change in admittance Y_{tbf} as recorded from the output of PSD
Y_t Total admittance of the general circuit shown in Fig. 1
Y_{tbf} Admittance of Y_{comp} and Y_1 in parallel; represents the total admittance Y_t before fusion occurs
ΔY_{tbf} Alteration in Y_{tbf} induced by a change in C_{m1}

Greek symbols

ω Angular frequency of the stimulating sine wave
ω_k Angular frequencies of both sine wave stimuli in MSW ($k = 1, 2$)
ϕ Argument of $T(\omega)$
φ Phase angle introduced by equipment and PSD
ω_1 Angular frequency of the first sine wave stimulus in MSW
$\varphi 1_{psd}$ Any φ_{psd} not equal to φ_{NM}
ω_2 Angular frequency of the second sine wave stimulus in MSW
φ_{eq} Phase shift introduced by equipment (but not PSD)
φ_{err} Error in the phase setting
φ_{NM} Phase set after NM approach was used
φ_{PL} Phase, satisfying requirements of PL technique
φ_{psd} Phase shift introduced by a PSD

INTRODUCTION

Admittance analysis of single small cells, introduced in the early 1980s to study exocytosis (Neher and Marty, 1982), remains a leading technique in the field of biological membrane fusion. This method, called *time-resolved admittance measurement* (TRAM) (Gillis, 1995), involves stimulating the cell with a sine wave in voltage, separating the in-phase and out-of-phase components of the resultant current by a phase-sensitive detector (PSD), and calculating the electrical parameters of an equivalent model circuit. Later, this model was augmented by an additional element, the fusion pore conductance (Zimmerberg et al., 1987), which explains a correlated wave of the in-phase component and a slow rise

in the out-of-phase component during each fusion event. More importantly, these admittance data led to the concept that membrane fusion occurs through the formation and widening of an initially narrow pore. Fusion pores were also measured by a direct current method, the "double whole-cell" recording (Lanzrein et al., 1993). Recently, comparison of the pore conductance measured by the direct current technique to that calculated using TRAM validated the model-dependent admittance analysis (Plonsky and Zimmerberg, 1996).

Since the invention of TRAM, different strategies for calculating the electrical parameters of fusing membranes have been suggested (see Lindau, 1991; Gillis, 1995, for reviews). The two most popular are the Lindau-Neher technique (LN) and the piecewise-linear technique (PL). In their initial form, both approaches neglect the fusion pore.

In LN, R_a, C_{m1}, and G_{m1} are computed while a cell is stimulated with a single sine wave superimposed on a holding potential, assuming that E_r is known and constant (symbols are cited in the legend to Fig. 1). A more general version of this technique uses a stimulus signal containing two sine waves with different frequencies, yielding calculation of R_a, C_{m1}, and G_{m1} without any restrictions on E_r (Rohlicek and Rohlicek, 1993; Donelly, 1994; Rohlicek and Schmid, 1994). Below, this generalized LN will be called the multiple sine wave method (MSW). The main problems facing both LN and MSW are phase offset and possible attenuation of current, caused by different pieces of equipment used in the experiment (amplifiers, filters, etc.).

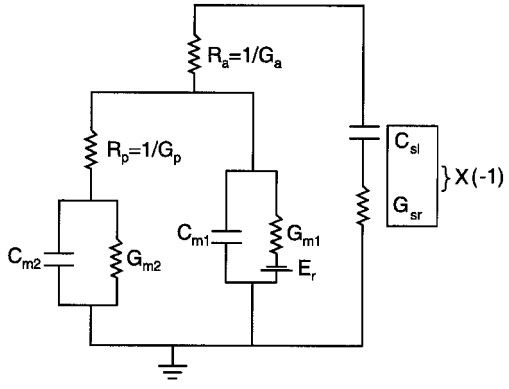

FIGURE 1 General equivalent circuit representing membrane fusion. Here R_a is the access (pipette) resistance, C_{m1} and R_{m1} are the capacitance and resistance of the first (patched and voltage-clamped) cell (or membrane), E_r is its resting potential, C_{m2} and R_{m2} are the capacitance and the resistance of the second initially nonclamped membrane (cell or intracellular granule), and R_p is the fusion pore resistance. C_{sl} and G_{sr} represent the C-slow and G-series potentiometers in the capacitance neutralization (compensation) circuitry of a patch-clamp amplifier. C_{sl} and G_{sr} in series are assumed to have a "negative" admittance Y_{comp}, which means that the addition of 1 pF in C_{sl} value will be seen as subtraction of 1 pF at the output of an amplifier. We denote the total admittance of the general circuit above as Y_t, the admittance of the first membrane as Y_{m1} (Y_{m1} consists of C_{m1}, G_{m1}, and E_r), and the admittance of the second membrane as Y_{m2} (Y_{m2} includes C_{m2} and G_{m2}). Y_{m1} in series with R_a forms Y_1, and Y_{m2} in series with G_p forms Y_2. Y_{m1+2} stands for the resulting admittance of Y_{m1} and Y_2 in parallel. Y_3 is the admittance of the general circuit without the compensation circuitry. Y_3 consists of R_a and Y_{m1+2} in series. Y_1 in parallel with Y_{comp} forms Y_{tbf}. Before fusion occurs, the left branch of the general circuit with the admittance Y_2 is not present, and the general circuit admittance reduces to Y_{tbf} (i.e., when $G_p = 0$, $Y_t = Y_{tbf}$).

PL requires compensation of R_a and C_{m1}, using the capacitance neutralization circuitry of a patch-clamp amplifier. Small changes in C_{m1} can be measured from the out-of-phase output of a PSD, provided the experimenter has set the correct phase angle, but calculation of elements other than C_{m1} is not available. The phase adjustment (Neher-Marty technique (NM); Neher and Marty, 1982) requires the operator to dither the amplifier's C-slow potentiometer while simultaneously changing the PSD phase angle. The correct phase angle is selected when C-slow-induced signals create maximum signals of the opposite sign in the PSD out-of-phase channel and no changes in the in-phase signal. PL also requires calibration of the out-of-phase channel, which is usually performed by displacing the C-slow potentiometer by a known value (a calibration "jump," which may require recalibration of the C-slow potentiometer). NM takes into account the phase offset introduced by equipment. Unfortunately, fluctuations of R_a and C_{m1} can occur in the course of an experiment, requiring an additional adjustment of the phase angle, for example, with the phase tracking technique (Joshi and Fernandez, 1988).

Below we describe how C-slow potentiometer jumps can be used both for the determination of phase shift and attenuation caused by experimental equipment and, by successive application of MSW, for calculation of parameters R_a, G_{m1}, and C_{m1}. We demonstrate how these jumps can be employed for an automatic setting of the correct phase angle in accordance with the Neher-Marty technique. Furthermore, we show how MSW can be modified for calculations of fusion pore conductance and the parameters G_{m2} and C_{m2} of the second (fusing) membrane.

MATERIALS AND METHODS

GP64, the baculovirus envelope protein that mediates membrane fusion during infection, has recently been shown to mediate fusion with human red blood cells (Leikina and Chernomordik, personal communication). A stably transfected Sf9 cell line expressing GP64 was a kind gift of Dr. Gary Blissard. For whole-cell recordings, solutions were (concentration in mM) 111 KGlu, 13.8 KCl, 1.7 $MgCl_2$, 8.5 HEPES, 4.3 EGTA, 43 sucrose, pH 7.2 with KOH, and pCa 8 with 0.71 mM $CaCl_2$ (internal), and 47.4 NaCl, 8.5 KCl, 3.4 $CaCl_2$, 4.3 $MgCl_2$, 4.3 glucose, 8.5 MES (2-[*N*-morpholino]ethanesulfonic acid; Sigma, St. Louis, MO), 163.8 sucrose, pH 6.2 with NaOH (external). Fusion was triggered with a highly buffered acidic solution (43 Na citrate, 43 NaCl, 8.5 KCl, 3.4 $CaCl_2$, 4.3 $MgCl_2$, 4.3 glucose, 17.2 sucrose, pH 5.0 with NaOH) delivered to Sf9/erythrocyte cell pairs by ejection from a micropipette. Patch pipettes had a resistance of 1–2 MΩ. The mean value of the access resistance shortly after the patch of membrane was ruptured was 4.6 MΩ.

TRAM was implemented in locally written software (*Browse*, available upon request). A 2-kHz, 50-mV peak-to-peak sine wave was superimposed on the holding potential (−20 mV). Sinusoidal current was filtered at 5 kHz with an 8-pole Bessel filter (Frequency Devices, Haverhill, MA), digitized at 40 kHz, and separated into in-phase and out-of-phase components (Joshi and Fernandez, 1988). Phase was set using automated NM (see

the Results for more details). Subsequently, the software output admittance, Y_{out}, was calculated by dividing the current by the stimulus sine wave amplitude. The fusion pore conductance, G_p, and the capacitance of the erythrocyte, C_{m2}, were calculated on the basis of the fusion-induced increment of Y_{out}, $(Y_{incr})_{out}$: $G_p = (R^2 + I^2)/[|T(\omega)|^2 R]$ and $C_{m2} = (R^2 + I^2)/[|T(\omega)|^2 \omega I]$ (Lindau, 1991). In these equations, R and I are the real and the imaginary components of $(Y_{incr})_{out}$, $\omega = 2\pi f$, f is the frequency of the stimulating sine wave, and $T(\omega)$ is the scaling factor. $T(\omega)$ was calculated as $1/(1 + j\omega C_{sl}/G_{sr})$, where C_{sl} and G_{sr} are settings of patch-clamp capacitance neutralization circuitry.

RESULTS

Outputs of a phase-sensitive detector do not represent pure real and imaginary components of the pipette-cell admittance

Let us first discuss the factors defining the signals recorded from the in-phase and out-of-phase channels of a PSD. (Below we always represent the in-phase and out-of-phase PSD signals as real and imaginary components of the source admittance.) Although the following analysis is not new, it will be needed below. Let A_{out} be the signal in-phase and B_{out} be the signal out-of-phase with respect to a stimulus signal with an angular frequency ω. Then the output complex admittance $Y_{out} = A_{out} + jB_{out}$, where $j = \sqrt{-1}$. The total admittance $Y_t = A_t + jB_t$, where A_t is the real and B_t is the imaginary component of Y_t (Fig. 1). Let us analyze the relationship between Y_t and Y_{out}.

Equipment (amplifiers, filters, etc.) introduces phase shifts into the circuit admittance by the frequency-dependent angle φ_{eq}, which results in the multiplication of Y_t by $\exp(j\varphi_{eq})$. For example, the 5-kHz 8-pole Bessel filter used in our experiments is the major phase-shifting source: it introduces $\varphi_{eq} = -72.3°$ ($f = 2$ kHz). Besides shifting the phase, the equipment may also cause some attenuation of the source admittance, resulting in the multiplication of Y_t by the constant $K > 0$. Thus the admittance at the input of the PSD, Y_{in}, will be

$$Y_{in} = A_{in} + jB_{in} = (A_t + jB_t)\exp(j\varphi_{eq})K. \quad (1)$$

The PSD usually has phase adjustment circuitry that allows a user to set the desirable phase angle. If we denote the phase shift introduced by a PSD as φ_{psd}, we have

$$Y_{out} = A_{out} + jB_{out} = (A_{in} + jB_{in})\exp(j\varphi_{psd}). \quad (2)$$

From Eqs. 1 and 2 we obtain

$$Y_{out} = (A_t + jB_t)\exp[j(\varphi_{eq} + \varphi_{psd})]K. \quad (3)$$

Whereas φ_{psd} is known during the experiment, φ_{eq} and K have to be determined to use LN and MSW. These methods consider the "true" admittance of the general circuit (Fig. 1). More accurately, they deal with its right-hand part, consisting of R_{m1}, C_{m1}, E_r, R_a, C_{sl}, and G_{sr}.

C-slow displacement can be used to restore the real and the imaginary components of the pipette and cell admittance to their true values

To calculate the compensation vector for restoration of Y_t, one can apply a signal with known amplitude and phase with respect to the stimulus sine wave (Donnelly, 1994). Below we consider the capacitance neutralization circuitry of a patch-clamp amplifier as a source of such a signal.

Suppose we are performing a "jump," increasing C_{sl} by a value ΔC_{sl}, starting from arbitrary values of G_{sr}, C_{sl}. The general circuit from Fig. 1 contains a combination of two membranes with the resulting admittance Y_3 in parallel with the compensation circuitry having "negative" admittance Y_{comp} (see Fig. 1 legend for more details). The admittance of the general circuit can thereby be represented as

$$Y_t = Y_3 - Y_{comp}. \quad (4)$$

If $G_p = 0$, Eq. 4 can be rewritten as $Y_{tbf} = Y_1 - Y_{comp}$ (Y_{tbf} and Y_1 are defined in the legend to Fig. 1). When a jump is being issued,

$$Y1_t = Y_3 - Y1_{comp}, \quad (5)$$

where $Y1_t$ is the new value of Y_t, and $Y1_{comp}$ is the new admittance of the compensation circuitry. Assuming that Y_3 does not change during the jump, from Eqs. 4 and 5 we easily obtain the next expression for the general circuit admittance change:

$$J = Y1_t - Y_t = Y_{comp} - Y1_{comp}. \quad (6)$$

Since C_{sl} is in series with G_{sr}, Y_{comp} can be calculated using the next equation:

$$Y_{comp} = G_{sr}j\omega C_{sl}/(G_{sr} + j\omega C_{sl}). \quad (7)$$

Similarly, for the admittance $Y1_{comp}$ we have

$$Y1_{comp} = G_{sr}j\omega(C_{sl} + \Delta C_{sl})/[G_{sr} + j\omega(C_{sl} + \Delta C_{sl})]. \quad (8)$$

Substituting the expressions for Y_{comp} and $Y1_{comp}$ into Eq. 6, we obtain

$$J = -j\omega\Delta C_{sl}/[(1 + j\omega C_{sl}/G_{sr})(1 + j\omega(C_{sl} + \Delta C_{sl})/G_{sr})]. \quad (9)$$

In the course of an experiment, instead of J we actually measure the phase-shifted and attenuated value J_{out}. According to the discussion above, J_{out} can be calculated using the following equation:

$$J_{out} = Y1_t\exp[j(\varphi_{eq} + \varphi_{psd})]K - Y_t\exp[j(\varphi_{eq} + \varphi_{psd})]K$$
$$= J\exp[j(\varphi_{eq} + \varphi_{psd})]K. \quad (10)$$

An important property of the jump-induced values J and J_{out} is their independence from the membrane parameters of the

general circuit.[1] The actual admittance change J depends only upon the magnitudes of G_{sr}, C_{sl}, and ΔC_{sl}, whereas the experimental value J_{out} is also determined by the characteristics of one's equipment (φ_{eq} and K) and the preset phase shift φ_{psd}.

Finally, the values of φ_{eq} and K can be calculated following the considerations below. From Eq. 10 we obtain

$$J_{out}/J = K \exp[j(\varphi_{eq} + \varphi_{psd}))]. \tag{11}$$

Now if C_{sl}, G_{sr}, and φ_{psd} are known, we can compute J from Eq. 9 and, using the experimental value J_{out}, calculate the attenuation K and equipment-originated phase shift φ_{eq} from Eq. 11. As we can see, the right part of Eq. 11 is just the polar representation of the complex number $Q = J_{out}/J$. Thus we have

$$\begin{aligned} K &= |Q|, \\ \varphi_{eq} + \varphi_{psd} &= \arg(Q), \end{aligned} \tag{12}$$

and consequently,

$$\varphi_{eq} = \arg(Q) - \varphi_{psd}. \tag{13}$$

If $Q = a + jb$, we can use the next two expressions for $\arg(Q)$:

$$\arg(Q) = \arctan(b/a), \quad \text{if } a > 0;$$

$$\arg(Q) = \arctan(b/a) + \pi, \quad \text{if } a < 0;$$

$$\arg(Q) = \pi/2, \quad \text{if } a = 0 \text{ and } b > 0;$$

$$\arg(Q) = -\pi/2, \quad \text{if } a = 0 \text{ and } b < 0.$$

[1]Let us consider the absolute value of J_{out}, which is used in the PL technique for the computation of small changes in the cell capacitance C_{m1}. From Eq. 10 we can derive

$$\begin{aligned} |J_{out}| &= |J \exp[j(\varphi_{eq} + \varphi_{psd})]K| = |J|K \\ &= K\omega\Delta C_{sl}/|(1 + j\omega C_{sl}/G_{sr})[1 + j\omega(C_{sl} + \Delta C_{sl})/G_{sr}]| \\ &= K\omega\Delta C_{sl}/([1 + (\omega C_{sl}/G_{sr})^2] \\ &\quad \cdot \{1 + [\omega(C_{sl} + \Delta C_{sl})/G_{sr}]^2\})^{1/2}. \end{aligned} \tag{F1}$$

From Eq. F1, assuming $K = 1$, we obtain

$$\begin{aligned} |J_{out}| &= \omega\Delta C_{sl}/([1 + (\omega C_{sl}/G_{sr})^2] \\ &\quad \cdot \{1 + [\omega(C_{sl} + \Delta C_{sl})/G_{sr}]^2\})^{1/2}. \end{aligned} \tag{F2}$$

The last equation shows that the absolute value of the jump can easily be calculated when the compensation parameters C_{sl} and G_{sr} are known. This equation also allows us to understand the nature of "calibration attenuation." Indeed, $|J_{out}|$ is less than the expected calibration-related increment of Y_t, which is equal to $\omega\Delta C_{sl}$. Equation F2 reveals that the ratio $\tau = |J_{out}|/(\omega\Delta C_{sl})$ is always less than 1, and the lapse between $|J_{out}|$ and $\omega\Delta C_{sl}$ increases with ω and is negligible when ωC_{sl} is much less than G_{sr}. For instance, for the compensation parameters $C_{sl} = 23$ pF, $\Delta C_{sl} = 1$ pF, and $G_{sr} = 0.2$ μS, τ is equal to 0.979 for $f = 200$ Hz and equals 0.647 for $f = 1000$ Hz.

Knowledge of the distortion parameters K and φ_{eq} allows us to transform the experimental admittance $Y_{out} = A_{out} + jB_{out}$ into the undistorted source admittance $Y_t = A_t + jB_t$. Using Eq. 3, we can come to the following formula:

$$\begin{aligned} Y_t = A_t + jB_t &= (A_{out} + jB_{out})/\{K \exp[j(\varphi_{eq} + \varphi_{psd})]\} \\ &= \exp[-j(\varphi_{eq} + \varphi_{psd})](A_{out} + jB_{out})/K. \end{aligned}$$

Or, if $G_p = 0$, the last equation can be rewritten as follows:

$$Y_{tbf} = \exp[-j(\varphi_{eq} + \varphi_{psd})](A_{out} + jB_{out})/K.$$

Compared to other techniques for restoration of the pipette and cell admittance, the above approach has obvious advantages. It does not require any additional hardware as suggested by Donelly (1994) or Rohlicek and Schmid (1994); nor does it need readjustments after filter or acquisition settings have been changed, such as those proposed by Gillis (1995).

Use of the restored value of cell-pipette admittance in the multiple sine wave algorithm

As soon as Y_t is restored, it becomes possible to obtain the true values of R_a, C_{m1}, and G_{m1}. For this purpose let us use MSW (Rohlicek and Rohlicek, 1993; Donnelly, 1994). In this case the stimulus signal consists of at least two sine waves, and the assumption $G_p = 0$ is made (i.e., $Y_t = Y_{tbf}$).

The calculation procedure looks as follows. Let ω_1 and ω_2 be frequencies incorporated in the stimulus signal, and $A_{tbf}(\omega_1) + jB_{tbf}(\omega_1)$ and $A_{tbf}(\omega_2) + jB_{tbf}(\omega_2)$ be the admittances of the general circuit corresponding to those frequencies. Using Eq. 4 in its rewritten form, and Eq. 7, we obtain

$$Y_1(\omega_k) = A_{tbf}(\omega_k) + jB_{tbf}(\omega_k) + Y_{comp} \tag{14}$$

and

$$Y_1(\omega_k) = A_{tbf}(\omega_k) + jB_{tbf}(\omega_k) + G_{sr}j\omega_k C_{sl}/(G_{sr} + j\omega_k C_{sl}),$$

where $k = 1, 2$ and $Y_1(\omega_k)$ is the admittance of the first (voltage-clamped) membrane circuitry, containing R_a, C_{m1}, G_{m1}, and E_r.

Now denoting $c_k + jd_k = Y_1(\omega_k)$, we can use the following generalizations of formulae from Donnelly (1994) to calculate R_a, C_{m1}, and G_{m1}:

$$\begin{aligned} R_a = (\omega_1 - \omega_2)/ \\ [(d_1 - d_2)(d_1\omega_1 - d_2\omega_2)/(c_1 - c_2) + c_1\omega_1 - c_2\omega_2], \end{aligned} \tag{15}$$

$$\begin{aligned} G_{m1} = (c_1 d_2\omega_2 - c_2 d_1\omega_1)/ \\ [d_2\omega_2 - d_1\omega_1 - R_a(c_1 d_2\omega_2 - c_2 d_1\omega_1)], \end{aligned} \tag{16}$$

$$\begin{aligned} C_{m1} = (c_2 - c_1)/ \\ \{R_a[d_2\omega_2 - d_1\omega_1 - R_a(c_1 d_2\omega_2 - c_2 d_1\omega_1)]\}. \end{aligned} \tag{17}$$

It is necessary to note that in Eqs. 15–17, $\omega_1 \neq 0$, $\omega_2 \neq 0$, and $\omega_1 \neq \omega_2$. However, these equations can be used even if one of the frequencies equals zero. In this case we should additionally assume that the resting potential is known and constant (see Gillis, 1995, for more details).

If both frequencies are greater than zero, Eqs. 15 and 16 can be used for the calculation of E_r. If several sine waves in the stimulus signal are superimposed on the holding potential (U_h), and I_h is the current generated by an amplifier to clamp the first membrane to U_h, we can easily obtain the following expression:

$$I_h R_a + I_h R_{m1} + E_r = U_h,$$

where $R_{m1} = 1/G_{m1}$. Now employing the value $G_{DC} = I_h/U_h$, we have $G_{DC}U_h(R_a + R_{m1}) + E_r = U_h$, and hence

$$E_r = U_h[1 - G_{DC}(R_a + 1/G_{m1})], \tag{18}$$

where R_a and G_{m1} are found from Eqs. 15 and 16 ($\omega_1 \neq 0$ and $\omega_2 \neq 0$).

The advantage of MSW is the ability to calculate C_{m1} at times when R_a and G_{m1} are also changing. Compared to the "phase tracking" technique (Joshi and Fernandez, 1988), which adjusts admittance measurement according to changes in R_a, MSW does not require any additional on-line actions, is free from deficiencies of phase tracking related to pipette capacitance (Gillis, 1995), and yields more information about cell parameters (E_r, R_a, and G_{m1}). Although dual-frequency methods are generally noisier than single-frequency techniques (Gillis, 1995), some new statistical approaches to reducing the estimation errors of the cell parameters were recently introduced (Barnett and Misler, 1997). We have shown that MSW can be improved by the incorporation of a new phase setting procedure, introduced in the previous section, yielding values of the pipette and cell admittance previously distorted by equipment.[2]

[2]MSW and the new phase setting procedure rely on readings of the C-slow and G-series potentiometers, for determination of Y_{comp} and φ_{eq}. These readings may be inaccurate (on the order of 5–10%) and introduce computational errors. Empirically, we found accurate calibration of these potentiometers to be of questionable value, because there was a nonlinear interaction between them, requiring the compilation of a look-up table containing all combinations of settings. Instead, we propose the following two-stage, "off-line playback" method to determine Y_{comp} and φ_{eq} when more accurate measurements are required. This procedure may also be used to accurately measure values of C_{sl} and G_{sr}. First, the value φ_{eq} is determined independently of C_{sl} and G_{sr} readings. For this purpose, the amplifier head-stage input is open to the air (disconnected), stray capacitance is compensated with the C-fast circuitry, and ΔC_{sl} is applied with settings of C_{sl} and G_{sr} that satisfy the following conditions: $\omega C_{sl} \ll G_{sr}$, $\omega \Delta C_{sl} \ll G_{sr}$. Then we can derive $J = -j\omega\Delta C_{sl}$ from Eq. 9, and obtain from Eq. 13

$$\varphi_{eq} = \arg(J_{out}/J) - \varphi_{psd} = \arg(J_{out}) - \arg(J) - \varphi_{psd} = \arg(J_{out}) + 3\pi/2 - \varphi_{psd}.$$

It is easy to see that this expression for φ_{eq} does not depend on the actual values C_{sl} and G_{sr}. For the second stage of this off-line playback procedure, the Y_{comp} value equal to the one produced by the compensation circuitry during each real experiment should be measured. For this purpose, the C_{sl} and G_{sr} potentiometers should be set to the values used in the experiment, and φ_{psd} should be set at $\varphi_{psd} = -\varphi_{eq}$, where φ_{eq} has been found as described here (we assume that the attenuation caused by equipment is negligible, so $K = 1$). Then the increment of the circuit admittance Y_{comp} should be measured by switching the C-slow circuitry off. When the input to the head stage of an amplifier is open, it is connected only to a "negative" admittance formed by the C-slow circuitry (see Fig. 1). Finally, this measured value Y_{comp} is used in Eq. 14 to find the value $Y_1(\omega_k)$ for Eqs. 15–17. Knowledge of Y_{comp} allows one to calculate accurate values of C_{sl} and G_{sr}, using formulae similar to Eqs. 51 and 52 described below. Note that MSW does not require the actual magnitudes of C_{sl} and G_{sr}, because only Y_{comp} is utilized in Eq. 14.

Proof of the validity of the empirical phase adjustments used in the "piecewise-linear" technique

Let us first derive the equation for the PL phase angle, $\varphi_{eq} + \varphi_{psd}$, which we denote as φ. Only φ_{psd} is experimentally adjustable, whereas φ_{eq} is constant. We assume that the attenuation caused by equipment is negligible, so $K = 1$. When $G_p = 0$, we can rewrite Eq. 3:

$$Y_{out} = A_{out} + jB_{out} = (A_{tbf} + jB_{tbf})\exp(j\varphi). \tag{19}$$

According to Lindau and Neher (1988), in this case a small change in C_{m1}, ΔC_{m1} induces the following alteration ΔY_{tbf} in Y_{tbf}:

$$\Delta Y_{tbf} = T(\omega)^2(A_{tbf} + j\omega\Delta C_{m1}). \tag{20}$$

Equation 20 holds true only if $G_a \gg G_{m1}$ and $G_a \approx \omega C_{m1}$ or $G_a > \omega C_{m1}$ (the sign $\approx$ in the last condition means "is comparable"). The factor $T(\omega)$ is calculated according to (Lindau, 1991)

$$T(\omega) = 1/(1 + G_{m1}/G_a + j\omega C_{m1}/G_a). \tag{21}$$

If $G_{m1} \ll G_a$,

$$T(\omega) = 1/(1 + j\omega C_{m1}/G_a). \tag{22}$$

Let $\Delta Y_{out}(\varphi)$ be the change in the output signal corresponding to a ΔC_{m1}-induced change ΔY_{tbf} in the admittance Y_{tbf}. We assume that the measurements are performed with the given phase φ. Then, from Eqs. 19 and 20,

$$\Delta Y_{out}(\varphi) = \Delta Y_{tbf}\exp(j\varphi) = T(\omega)^2(A_{tbf} + j\omega\Delta C_{m1})\exp(j\varphi).$$

Let ϕ be the argument of $T(\omega)$. Then $T(\omega) = |T(\omega)|\exp(j\phi)$, and we can rewrite the previous expression for $\Delta Y_{out}(\varphi)$:

$$\Delta Y_{out}(\varphi) = |T(\omega)|^2\exp[j(2\phi + \varphi)](A_{tbf} + j\omega\Delta C_{m1}). \tag{23}$$

The PL technique assumes that the phase φ is chosen such that

$$2\phi + \varphi = 0 \tag{24}$$

(Lindau and Neher, 1988). Indeed, denoting the phase φ (satisfying Eq. 24) as φ_{PL},

$$\varphi_{PL} = -2\phi = -2\arg(T(\omega)) = -2\arg[1/(1 + j\omega C_{m1}/G_a)]. \tag{25}$$

From Eq. 23, $\Delta Y_{out}(\varphi) = |T(\omega)|^2(A_{tbf} + j\omega\Delta C_{m1})$, and for the imaginary part of $\Delta Y_{out}(\varphi)$ we have $\mathrm{Im}(\Delta Y_{out}(\varphi)) = |T(\omega)|^2\omega\Delta C_{m1}$. Thus small changes in the imaginary part of the admittance are recorded from the out-of-phase channel of a PSD. Notice that φ_{PL} is determined by the cell "circuitry," but not by compensation parameters.

Now, having derived Eq. 25 for the phase angle used in PL, we will describe how the phase is actually set in NM and investigate when this value of φ satisfies Eq. 24. We first derive an equation describing changes in the general admittance induced by displacements of the potentiometer C-slow. Using Eqs. 9 and 10 and assuming $K = 1$, we obtain the following formula:

$$J_{out} = (-j\omega\Delta C_{sl}/\{(1 + j\omega C_{sl}/G_{sr})[1 + j\omega(C_{sl} + \Delta C_{sl})/G_{sr}]\}) \cdot \exp(j\varphi). \quad (26)$$

The phase in NM is set to allow J_{out} to be represented by a vector going downward along the imaginary axis, which means that $\arg(J_{out}) = 3\pi/2$. Let us denote this phase value as φ_{NM}. Because multiplication (division) of complex numbers adds (subtracts) their arguments, we have from Eq. 26

$$3\pi/2 = \arg(J_{out}) = \arg(-j\omega\Delta C_{sl}) + \varphi_{NM} - \arg\{(1 + j\omega C_{sl}/G_{sr})[1 + j\omega(C_{sl} + \Delta C_{sl})/G_{sr}]\}.$$

Because $\arg(-j\omega\Delta C_{sl}) = 3\pi/2$, we obtain from the previous equation

$$\varphi_{NM} = \arg(1 + j\omega C_{sl}/G_{sr}) + \arg[1 + j\omega(C_{sl} + \Delta C_{sl})/G_{sr}]. \quad (27)$$

Note that unlike φ_{PL}, φ_{NM} is determined by elements of the neutralization circuitry.

Now we can determine if φ_{NM} satisfies Eq. 24. In addition to earlier assumptions that ($G_a \gg G_{m1}$, $G_a > \omega C_{m1}$ or $G_a \approx \omega C_{m1}$), we will need the next three: $C_{sl} \cong C_{m1}$, $G_{sr} \cong G_a$, and $\Delta C_{sl} \ll C_{sl}$. Based on all of these assumptions, we have from Eq. 27

$$\varphi_{NM} = 2\arg(1 + j\omega C_{sl}/G_{sr}) = 2\arctan(\omega C_{sl}/G_{sr}) = 2\arctan(\omega C_{m1}/G_a). \quad (28)$$

From Eq. 25 we can easily obtain φ_{PL}:

$$\varphi_{PL} = -2\arg[1/(1 + j\omega C_{m1}/G_a)] = 2\arg(1 + j\omega C_{m1}/G_a) = 2\arctan(\omega C_{m1}/G_a) = \varphi_{NM}.$$

This proves our point: when $\varphi = \varphi_{NM}$, the phase angle satisfies the requirement of PL. This statement holds true as long as $C_{sl} \cong C_{m1}$ and $G_{sr} \cong G_a$. The assumptions $C_{sl} \cong C_{m1}$ and $G_{sr} \cong G_a$ are true immediately after the compensation has been performed, because it is possible to show that for a single cell the compensation parameters satisfy the next two equations (Lindau and Neher, 1988):

$$C_{sl} \cong C_{m1}(1 - 2R_a/R_{m1}), \quad (29)$$

$$G_{sr} \cong G_a(1 - R_a/R_{m1}). \quad (30)$$

If $G_a \gg G_{m1}$, we can easily produce the necessary conditions $C_{sl} \cong C_{m1}$ and $G_{sr} \cong G_a$ from Eqs. 29 and 30.

This analytical proof of the validity of the empirical phase adjustments used in PL replaces the assertion that C_{sl} is equivalent to C_{m1} (Lindau and Neher, 1988).

Finally, using Eq. 10, we introduce an algorithm for quickly determining the PSD phase shift according to NM. Suppose a calibration jump routinely used in NM to determine the scaling factor $|T(\omega)|^2$ is made when $\varphi_{psd} = \varphi_{NM}$. Assuming $K = 1$, from Eq. 10 we have:

$$J_{out} = J\exp[j(\varphi_{eq} + \varphi_{NM})],$$

and

$$3\pi/2 = \arg(J_{out}) = \arg(J) + \varphi_{eq} + \varphi_{NM}. \quad (30a)$$

If the same jump is made when $\varphi_{psd} = \varphi 1_{psd} \neq \varphi_{NM}$, where $\varphi 1_{psd}$ is known and the output signal $J1_{out}$ is measured, we have

$$J1_{out} = J\exp[j(\varphi_{eq} + \varphi 1_{psd})]$$

and

$$\arg(J1_{out}) = \arg(J) + \varphi_{eq} + \varphi 1_{psd}.$$

Subtracting the last equation from Eq. 30a, we have $3\pi/2 = \arg(J1_{out}) = \varphi_{NM} - \varphi 1_{psd}$. This gives us the next simple expression, which can be implemented in the software to adjust phase according to NM:

$$\varphi_{NM} = \varphi 1_{psd} + 3\pi/2 - \arg(J1_{out}).$$

Thus a calibration jump can yield the phase. The dithering of potentiometers required in NM can be completely avoided, saving valuable time in the course of an experiment. Note that the described algorithm for finding φ_{NM} is independent of the readings of the compensation potentiometers (see footnote 2).

Fusion pore calculation algorithms: initial considerations

We will now describe some algorithms for calculation of elements of an equivalent circuit for membrane fusion (Fig. 1), primarily, the fusion pore conductance. The fusing circuitry consists of G_p, C_{m2}, and G_{m2}, and has admittance Y_2. Therefore, calculation of G_p, C_{m2}, and G_{m2} is based on the determination of Y_2.

Before fusion, there is no electrical contact between the two membrane systems ($G_p = 0$), so the circuit is represented by R_a, C_{m1}, G_{m1}, E_r, C_{sl}, and G_{sr} and has admittance Y_{tbf}. The in-phase and out-of-phase signals from a PSD at this time comprise the base line and are usually subtracted from the admittance of the general circuit when fusion has occurred ($G_p > 0$). Let us assume, during the entire process of fusion pore formation, constancy of the parameters R_a, G_{m1}, and C_{m1} of the patch-clamped membrane, and of the compensation parameters C_{sl} and G_{sr}. Unlike Lindau (1991), we will not require either C_{m2} or G_{m2} to be constant.

Now for the base line admittance we obtain, using the rewritten form of Eq. 4,

$$Y_{tbf} = Y_1 - Y_{comp} = G_a Y_{m1}/(G_a + Y_{m1}) - Y_{comp}, \quad (31)$$

where Y_{m1} denotes the admittance of the patch-clamped membrane with elements C_{m1}, G_{m1}, and E_r; Y_1 stands for the resulting admittance of Y_{m1} and R_a in series. If we use sine wave stimulation with the frequency $\omega > 0$, we can ignore the resting potential E_r. In this case $Y_{m1} = G_{m1} + j\omega C_{m1}$, because this part of the general circuit contains just C_{m1} and G_{m1} in parallel. Let us denote $Y_{m2} = G_{m2} + j\omega C_{m2}$ as the admittance of the second membrane, and Y_2 as the resulting admittance of Y_{m2} and G_p in series. As in Eq. 31, the total admittance Y_t of the circuit in the general case ($G_p > 0$) can be written as

$$Y_t = Y_3 - Y_{comp} = G_a Y_{m1+2}/(G_a + Y_{m1+2}) - Y_{comp}, \quad (32)$$

where Y_3 includes R_a and Y_{m1+2} in series, and $Y_{m1+2} = Y_{m1} + Y_2$, because Y_{m1} is in parallel with Y_2. Now from Eqs. 31 and 32, the fusion-related increment of the total admittance, Y_{incr}, is

$$\begin{aligned} Y_{incr} &= Y_t - Y_{tbf} \\ &= (Y_3 - Y_{comp}) - (Y_1 - Y_{comp}) \\ &= Y_3 - Y_1 \\ &= G_a Y_{m1+2}/(G_a + Y_{m1+2}) - G_a Y_{m1}/(G_a + Y_{m1}). \end{aligned} \quad (33)$$

Substituting Y_{m1} with $G_{m1} + j\omega C_{m1}$, we obtain from Eq. 33

$$\begin{aligned} Y_{incr} = {} & G_a(G_{m1} + j\omega C_{m1} + Y_2)/(G_a + G_{m1} + j\omega C_{m1} + Y_2) \\ & - G_a(G_{m1} + j\omega C_{m1})/(G_a + G_{m1} + j\omega C_{m1}) \end{aligned}$$

or

$$Y_{incr} = T(\omega) Y_2/[1/T(\omega) + Y_2/G_a], \quad (34)$$

where $T(\omega)$ is defined in Eq. 21.

Because Y_2 is a series sequence of G_p and parallel combination of G_{m2} and C_{m2},

$$Y_2 = G_p(G_{m2} + j\omega C_{m2})/(G_p + G_{m2} + j\omega C_{m2}). \quad (35)$$

The expression above leads to the following inequality[3]:

$$|Y_2/G_a| \le \min(G_p/G_a, |(G_{m2} + j\omega C_{m2})/G_a|). \quad (36)$$

From Eq. 36 it can easily be seen that we can neglect the ratio Y_2/G_a in Eq. 34, if any of the next two conditions is true: $G_p \ll G_a$, or $G_{m2} \ll G_a$ and $\omega C_{m2} \ll G_a$. If this is the case, we can simplify the expression for Y_{incr}, given in Eq. 34:

$$Y_{incr} = T(\omega)^2 Y_2. \quad (37)$$

From Eq. 3 one can see that in the course of an experiment with the phase shift $\varphi = \varphi_{eq} + \varphi_{psd}$ and attenuation K, the measured fusion-induced increment of the total admittance, $(Y_{incr})_{out}$, is equal to

$$\begin{aligned} (Y_{incr})_{out} &= KY_t \exp(j\varphi) - KY_{tbf}\exp(j\varphi) \\ &= K(Y_t - Y_{tbf})\exp(j\varphi) = Y_{incr}\exp(j\varphi)K. \end{aligned}$$

Representing $T(\omega) = |T(\omega)|\exp(j\phi)$, where $\phi = \arg(T(\omega))$, using Eq. 37, and assuming that either $K = 1$ or a corresponding correction has been performed according to Eq. 12, we have

$$\begin{aligned} (Y_{incr})_{out} &= T(\omega)^2 Y_2 \exp(j\varphi) = |T(\omega)|^2 \exp(2j\phi) Y_2 \exp(j\varphi) \\ &= Y_2 |T(\omega)|^2 \exp[j(\varphi + 2\phi)]. \end{aligned}$$

From the last equation we obtain

$$Y_2 = (Y_{incr})_{out}\exp[-j(\varphi + 2\phi)]/|T(\omega)|^2. \quad (38)$$

We have derived an important equation, showing the relationship between the fusion-related signal $(Y_{incr})_{out}$ from the PSD and the admittance of the fusing circuitry, containing G_p, G_{m2}, and C_{m2}.

Below we describe two different approaches that both allow reconstruction of Y_2 from Eq. 38 and its subsequent utilization for finding G_p, G_{m2}, and C_{m2}, which determine Y_2 according to Eq. 35. In the first reconstruction approach, the phase is directly calculated using C-slow jumps. The experimenter performs a C-slow displacement and then triggers fusion. For further calculation during off-line analysis, one should use a part of the base line immediately preceding fusion. Exploiting the algorithm described above, the magnitudes of φ_{eq}, φ, and $T(\omega)$-determining parameters R_a, C_{m1}, and G_{m1} can be obtained from Eqs. 13, and 15–17.

[3]From Eq. 35 we have

$$Y_2/G_a = (G_p/G_a)(G_{m2} + j\omega C_{m2})/(G_p + G_{m2} + j\omega C_{m2})$$

and

$$\begin{aligned} |Y_2/G_a| &= |(G_p/G_a)(G_{m2} + j\omega C_{m2})/(G_p + G_{m2} + j\omega C_{m2})| \\ &= (G_p/G_a)|(G_{m2} + j\omega C_{m2})/(G_p + G_{m2} + j\omega C_{m2})|. \end{aligned}$$

$|Y_2/G_a| \le G_p/G_a$, because $|(G_{m2} + j\omega C_{m2})/(G_p + G_{m2} + j\omega C_{m2})|$ is equal to 1 when $G_p = 0$ and is less than 1 when $G_p > 0$. Similarly, we obtain from Eq. 35,

$$Y_2/G_a = [(G_{m2} + j\omega C_{m2})/G_a]G_p/(G_p + G_{m2} + j\omega C_{m2})$$

and

$$\begin{aligned} |Y_2/G_a| &= |(G_{m2} + j\omega C_{m2})/G_a||G_p/(G_p + G_{m2} + j\omega C_{m2})| \\ &\le |(G_{m2} + j\omega C_{m2})/G_a|, \end{aligned}$$

because

$$|G_p/(G_p + G_{m2} + j\omega C_{m2})| \le 1.$$

Thus we have: $|Y_2/G_a| \le \min(G_p/G_a, |(G_{m2} + j\omega C_{m2})/G_a|)$.

Then one can calculate $T(\omega)$ from Eq. 21, and find $\phi = \arg[T(\omega)]$ and the factor $\exp[-j(\varphi + 2\phi)]/|T(\omega)|^2$. Because, according to our previous assumptions, R_a, C_{m1}, and G_{m1} do not change after fusion occurs, the experimenter then can restore Y_2 from the distorted signal $(Y_{incr})_{out}$, using Eq. 38.

The second approach assumes that the phase has been set using the manual or automated Neher-Marty technique (i.e., $\varphi = -2\phi$). In this case we can conclude from Eqs. 38 and 24:

$$Y_2 = (Y_{incr})_{out}/|T(\omega)|^2. \tag{39}$$

The second approach is more "demanding": it requires correct compensation of G_a and C_{m1} for the entire experiment, whereas the first approach implies only the constancy of these parameters. If R_a or C_{m1} has changed and reached a new level between fusion triggering and pore formation (which is quite possible, because a delay between triggering and fusion can be as long as 217 s; Zimmerberg et al., 1994), only the first approach gives the correct results. Therefore, the first approach is "safer." However, the calculations in the second case are less complicated, because only $|T(\omega)|^2$ has to be found for the restoration of Y_2.[4] Another advantage of the second approach is its independence from the readings of the compensation potentiometers, which can introduce additional errors (see footnote 2).

Both Y_2 reconstruction approaches discussed in this section provide us with at least one equation of the type

$$Y_2 = A_2 + jB_2 \tag{40}$$

where A_2 and B_2 are known and can be used to construct and resolve the equations with respect to G_p and, in some cases, with respect to parameters C_{m2} and G_{m2} of the second membrane. In the next section we will examine different algorithms for the calculation of these parameters. Each of the algorithms will be based on specific assumptions and sets of in-phase and out-of-phase signals obtained from a PSD.

Using the modified multiple sine wave approach for calculation of the parameters of the second membrane

Although MSW was initially designed for the analysis of the first membrane (G_p was neglected), it can be used for calculations of parameters included in the fusing circuitry, comprising G_p, C_{m2}, and G_{m2}. Using a stimulus signal containing two different sine waves with frequencies $\omega_1 \neq \omega_2$, we will try to determine all three parameters, G_p, G_{m2}, and C_{m2}. In this case Eq. 40 can be rewritten as follows:

$$Y_2(\omega_k) = A_2(\omega_k) + jB_2(\omega_k), \qquad k = 1, 2. \tag{41}$$

Here we actually have the classical Lindau-Neher model, where instead of the circuitry containing G_a, C_{m1}, and G_{m1}, a functionally identical circuitry with the corresponding parameters G_p, C_{m2}, and G_{m2} becomes apparent. Using Eqs. 15–17, making the substitutions $G_p \rightarrow G_a$, $G_{m2} \rightarrow G_{m1}$, $C_{m2} \rightarrow C_{m1}$, and denoting $A_2(\omega_k) = g_k$ and $B_2(\omega_k) = h_k$ ($k = 1, 2$), we obtain

$$G_p = [(h_1 - h_2)(h_1\omega_1 - h_2\omega_2)/(g_1 - g_2) + g_1\omega_1 - g_2\omega_2]/(\omega_1 - \omega_2), \tag{42}$$

$$G_{m2} = (g_1h_2\omega_2 - g_2h_1\omega_1)/[h_2\omega_2 - h_1\omega_1 - (g_1h_2\omega_2 - g_2h_1\omega_1)/G_p], \tag{43}$$

$$C_{m2} = (g_2 - g_1)G_p /[h_2\omega_2 - h_1\omega_1 - (g_1h_2\omega_2 - g_2h_1\omega_1)/G_p]. \tag{44}$$

If the first approach for $Y_2(\omega_k)$ reconstruction is applied as described in the previous section, g_k and h_k are calculated from the PSD signals, and therefore G_p, G_{m2}, and C_{m2} can be determined.

Let us consider the phase adjusted with the Neher-Marty technique as described above. We will denote the real and imaginary parts of the measured admittance increment $(Y_{incr})_{out}$ for the frequency ω_k as R_k and I_k, so that

$$[Y_{incr}(\omega_k)]_{out} = R_k + jI_k, \tag{45}$$

where $k = 1, 2$. In this case, according to Eq. 39,

$$g_k = R_k/|T(\omega_k)|^2, \qquad h_k = I_k/|T(\omega_k)|^2, \tag{46}$$

where $|T(\omega_k)|^2$ can be found by employing Eqs. F3 or F4 from footnote 4. Substituting the values g_k and h_k from Eq.

---

[4] To calculate Y_2 according to Eq. 39, the conditions $C_{sl} \cong C_{m1}$, $G_{sr} \cong G_a$, and $\Delta C_{sl} \ll C_{sl}$ have to be satisfied. Then the coefficient $|T(\omega)|^2$ can be calculated from Eq. 22, using the approximations of G_a and C_{m1} by the compensation parameters G_{sr} and C_{sl}:

$$\begin{aligned} |T(\omega)|^2 &= |1/(1 + j\omega C_{m1}/G_a)|^2 \\ &= 1/[1 + (\omega C_{m1}/G_a)^2] \\ &= 1/[1 + (\omega C_{sl}/G_{sr})^2]. \end{aligned} \tag{F3}$$

If the compensation parameters are unknown, $|T(\omega)|^2$ can still be found. Because $\Delta C_{sl} \ll C_{sl}$, we obtain from Eq. F2 (footnote 1)

$$\begin{aligned} &|J_{out}|/(\omega\Delta C_{sl}) \\ &\quad = 1/([1 + (\omega C_{sl}/G_{sr})^2]\{1 + [\omega(C_{sl} + \Delta C_{sl})/G_{sr}]^2\})^{1/2} \\ &\quad \cong 1/\{[1 + (\omega C_{sl}/G_{sr})^2]^2\}^{1/2} = 1/[1 + (\omega C_{sl}/G_{sr})^2] \\ &\quad = |T(\omega)|^2. \end{aligned} \tag{F4}$$

Thus $|T(\omega)|^2$ can be approximated by the ratio of absolute values of experimental and expected calibration jumps, provided that the calibration took place when $G_p = 0$, and that necessary assumptions ($G_a \gg G_{m1}$, $G_a > \omega C_{m1}$ or $G_a \approx \omega C_{m1}$, $C_{sl} \cong C_{m1}$, $G_a \cong G_a$, and $\Delta C_{sl} \ll C_{sl}$) were all true. Furthermore, for the truthfulness of Eq. 39, either the condition $G_p \ll G_a$ or both conditions, $G_{m2} \ll G_a$ and $\omega C_{m2} \ll G_a$, should be satisfied. If we additionally require that $\omega C_{m1} \ll G_a$, we can approximate $|T(\omega)|^2$ as 1, and Eq. 39 can be further simplified:

$$Y_2 = (Y_{incr})_{out}. \tag{F5}$$

46 into Eqs. 42–44, we can calculate G_p, C_{m2}, and G_{m2}. No matter which reconstruction approach is used, this modified MSW yields G_{m2}, which has been neglected by previously published methods.

Single sine wave approach: calculation of G_p and C_{m2} using two channels of a PSD

Now let us consider a single sine wave of frequency ω contained in the stimulus signal, and make an additional assumption that G_{m2} is negligible compared to ωC_{m2}. Then we can safely assume that $G_{m2} = 0$ and obtain from Eq. 35

$$\begin{aligned} Y_2 &= G_p j\omega C_{m2}/(G_p + j\omega C_{m2}) \\ &= G_p j\omega C_{m2}(G_p - j\omega C_{m2})/[G_p^2 + (\omega C_{m2})^2] \\ &= G_p(\omega C_{m2})^2/[G_p^2 + (\omega C_{m2})^2] + jG_p^2\omega C_{m2}[G_p^2 \\ &\quad + (\omega C_{m2})^2]. \end{aligned} \tag{47}$$

If $Y_2 = A_2 + jB_2$, where A_2 and B_2 are known real and imaginary parts of the admittance of the circuitry containing G_p and C_{m2},

$$A_2 = G_p(\omega C_{m2})^2/[G_p^2 + (\omega C_{m2})^2], \tag{48}$$

$$B_2 = G_p^2\omega C_{m2}/[G_p^2 + (\omega C_{m2})^2], \tag{49}$$

then

$$A_2^2 + B_2^2 = G_p^2(\omega C_{m2})^2/[G_p^2 + (\omega C_{m2})^2]. \tag{50}$$

Dividing Eq. 50 by Eqs. 48 and 49, we obtain

$$G_p = (A_2^2 + B_2^2)/A_2, \tag{51}$$

$$C_{m2} = (A_2^2 + B_2^2)/\omega B_2. \tag{52}$$

The first approach to the reconstruction of Y_2 allows calculations of A_2 and B_2 from PSD signals. Then we can employ Eqs. 51 and 52 to find the values of G_p and C_{m2}. (This approach can be applied only if a stimulus sine wave is superimposed on a holding potential, and E_r is known and constant.)

If the PSD phase has been adjusted using NM, the admittance increment $(Y_{incr})_{out} = R + jI$ can be used instead of A_2 and B_2 in Eqs. 51 and 52. According to Eq. 39,

$$A_2 = R/|T(\omega)|^2 \tag{53}$$

and

$$B_2 = I/|T(\omega)|^2. \tag{54}$$

Substituting these expressions for A_2 and B_2 into Eqs. 51 and 52, we obtain

$$G_p = (R^2 + I^2)/(R|T(\omega)|^2), \tag{55}$$

$$C_{m2} = (R^2 + I^2)/(\omega I|T(\omega)|^2), \tag{56}$$

where $|T(\omega)|^2$ is calculated according to Eq. F3 or F4 (footnote 4). Thus, having one sine wave in the stimulus signal and employing the signals from both channels of a PSD, we can find G_p and C_{m2}. If we substitute the expression for Y_2 from Eq. 47 into Eq. 37, then for Y_{incr} we will come to the formula identical to equation 21 of Lindau (1991). Our Eq. 56 in the particular case $|T(\omega)|^2 = 1$ has also been derived by Lindau (1991, equation 23).

In the previous two sections we considered two approaches for finding parameters of the second (fusing) membrane. The modified MSW approach is more general, because it does not assume that G_{m2} is negligible with respect to ωC_{m2}. This might be the case when low-frequency measurements are required or when the second membrane is excitable or leaky because of viral infection. However, the single sine wave approach is sometimes more practical, because it does not require a second sine wave and it can be used with an analog lock-in amplifier. The modified MSW approach requires more parameters and operations and thus can be disadvantageous when significant measurement errors occur.

Any implementation of these algorithms should take into account the effect of noise on nonlinear calculations based upon PSD measurements, as described in Zimmerberg (1993) for single-channel fusion pore calculations. One must exclude from the determination of the parameters of the second membrane not only the extremes for which the calculation formula are inapplicable, but also parts of an experiment in which the data lie inside so-called noise bounds around these extreme points, where the parameters of the second membrane should be considered undefined. (This approach has been implemented in the software *Browse* (see Materials and Methods). For instance, while calculating C_{m2} according to Eq. 56, the software considers C_{m2} undefined not only when $I = 0$, but also in situations when I is small enough (does not exceed some multiple of the standard deviation of the imaginary channel calculated for the base line interval).) In such situations, having many different calculation procedures becomes especially valuable, because different algorithms generally have different "informationally undefined" areas, and an experimenter might be able to apply one algorithm to some intervals of data for which other algorithms do not work. For instance, if values g_1 and g_2 in Eq. 42 were close to each other, MSW would not work, because this equation contains their difference as a divider. On the other hand, application of the single sine wave method could still be possible in this case.

Pore conductance can be calculated even if G_{m1} changes in the course of an experiment

There are situations in which G_{m1} is not constant during fusion. In the above calculations of Y_{incr}, we denote the new conductance of the patch-clamped membrane when $G_p > 0$ as $G1_{m1} = G_{m1} + \Delta G_{m1}$. In this case, the admittance Y_{m1+2} of the parallel combination of the first and the second membranes can be expressed as

$$Y_{m1+2} = G_{m1} + \Delta G_{m1} + j\omega C_{m1} + Y_2.$$

Substituting this expression into Eq. 33 and denoting $Y_2 + \Delta G_{m1}$ as Y_G, we obtain

$$Y_{incr} = G_a(G_{m1} + j\omega C_{m1} + Y_G)/(G_a + G_{m1} + j\omega C_{m1} + Y_G) - G_a(G_{m1} + j\omega C_{m1})/(G_a + G_{m1} + j\omega C_{m1}).$$

This expression reduces to an equation that looks identical to Eq. 34 with respect to Y_G:

$$Y_{incr} = T(\omega)Y_G/(1/T(\omega) + Y_G/G_a). \quad (57)$$

If one of the two conditions below is true, we can neglect the ratio Y_G/G_a:

$$G_p \ll G_a \quad \text{and} \quad \Delta G_{m1} \ll G_a,$$

or

$$G_{m2} \ll G_a,\ \omega C_{m2} \ll G_a, \quad \text{and} \quad \Delta G_{m1} \ll G_a.$$

Then

$$Y_{incr} = T(\omega)^2 Y_G. \quad (58)$$

Let us restrict ourselves to the second approach of Y_2 restoration described above. We can then derive an equation similar to Eq. 39:

$$Y_G = (Y_{incr})_{out}/|T(\omega)|^2. \quad (59)$$

Denoting $(Y_{incr})_{out} = R + jI$, we have

$$Y_2 = (R + jI)/|T(\omega)|^2 - \Delta G_{m1}. \quad (60)$$

If G_{m2} is negligible and E_r is known and constant, exploiting the value $G_{DC} = I_h/U_h$ we can still use Eq. 18, even when the left part of the general circuit is present ($G_p > 0$). From Eq. 18 we have

$$G_{DC}(1/G_a + 1/G_{m1}) = (U_h - E_r)/U_h. \quad (61)$$

Because we have assumed that $G_a \gg G_{m1}$, from Eq. 61 we can conclude that

$$Gl_{m1} = G_{DC}U_h/(U_h - E_r). \quad (62)$$

Using Eq. 62, we can calculate the change ΔG_{m1} in the Gl_{m1} value, then employ Eq. 60 and single or multiple sine wave algorithms for calculation of fusion pore G_p and (optionally) the capacitance C_{m2}. In the particular case, when $G_a \gg \omega C_{m1}$, we can assume $|T(\omega)|^2 \cong 1$. Then from Eq. 60 we have

$$Y_2 = (R - \Delta G_{m1}) + jI.$$

This last equation is similar to Eq. F5 from footnote 4. It shows that when G_{m1} changes and $|T(\omega)|^2 \cong 1$, rather than the pure in-phase signal of the PSD, we can simply use its adjusted value, $R - \Delta G_{m1}$.

Practical considerations

In systems where membrane fusion during exocytosis can be recorded at the level of a single event, a noninstantaneous increase in capacitance reflects the gradual expansion of a fusion pore (Zimmerberg et al., 1987). However, if capacitance is calculated on the basis of signals from both output channels of PSD, its true steplike shape can be restored (Lindau, 1991). Here we show that when G_p is small, and the frequency of the stimulating sine wave is high, such restoration is extremely sensitive to any phase errors. (The effect of small phase errors on the estimation of single cell parameters under the condition of a large decaying membrane conductance was recently investigated by Barnett and Misler (1997).) Let us assume that we have the following values of the elements of our general circuit: $f = 2$ kHz, $R_a = 4.8$ MΩ, $G_{m1} = G_{m2} = 0$, $C_{m1} = 16.6$ pF, and $C_{m2} = 1$ pF. These values are characteristic of studies on virus-induced cell-cell fusion, which we discuss below. Suppose that the PSD signals reflect the admittance $Y_2 = A_2 + jB_2$, shifted by an angle φ_{err}:

$$(Y_2)_{out} = Y_2\exp(j\varphi_{err}) = A_{err} + jB_{err}.$$

Substituting A_{err} and B_{err} into Eqs. 51 and 52, we obtain

$$C_{err} = (A_{err}^2 + B_{err}^2)/\omega B_{err} \quad (63)$$

and

$$G_{err} = (A_{err}^2 + B_{err}^2)/A_{err}, \quad (64)$$

where C_{err} and G_{err} are values of C_{m2} and G_p, distorted because of φ_{err}. If we assume that G_p linearly increases from 1 to 100 nS, we can analyze how calculations of these two parameters are affected by a phase offset. Fig. 2 *A* demonstrates that when G_p is small, even a 2°–3° error in the phase settings can introduce substantial distortions of C_{m2}. Such errors could be expected in practice, simply because the phase is always adjusted before fusion occurs. Fortunately, while the pore widens, the C_{m2} computation error vanishes. On the contrary, G_{err} deviates from G_p only after substantial pore widening, indicating that we can safely measure small pores when the phase is not perfect (Fig. 2 *B*).

From Eq. 48 one can conclude that when the pore is narrow and the phase is set just about right, B_2 is very small. Under these conditions, any deviations in phase introduce substantial errors in C_{m2} because B_{err} is a part of the denominator of Eq. 63. When the pore is large, A_2 turns small, and the calculation of G_p becomes sensitive to phase errors because of A_{err} in the denominator of Eq. 64.

The phase sensitivity of the algorithm for the calculation of C_{m2} explains some phenomena observed in practice. Experiments, shown in Fig. 3, were performed to study fusion between GP64-bearing insect cells and erythrocytes. Automated NM was used for phase adjustments; G_p and C_{m2} were calculated on the basis of two channels of the phase-sensitive software according to Eqs. 55 and 56. Red blood cells have a capacitance of ~1 pF. When the phase was set correctly, the C_{m2} trace rose almost instantaneously, i.e., it had a steplike shape (Fig. 3 *A*). However, usually the C_{m2} trace was distorted because of a phase offset.

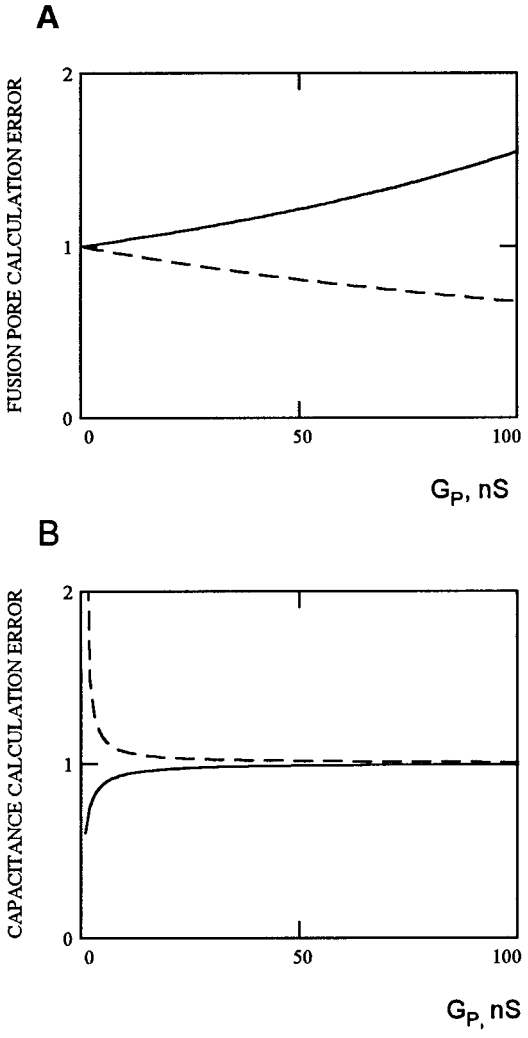

FIGURE 2 Computer simulations of the calculation errors induced by incorrect phase offsets. Calculations of C_{m2} (*A*) and G_p (*B*) were performed assuming that $(Y_2)_{out}$ (the measured value of the fusing circuitry admittance) deviates from Y_2 because of a phase offset (φ_{err}). The values of the real and the imaginary components of $(Y_2)_{out}$ were computed, and distorted values of G_p, C_{m2} (G_{err}, C_{err}, respectively) were recalculated according to Eqs. 63 and 64. Phase-related errors were found by dividing C_{err} by C_{m2} and G_{err} by G_p; φ_{err} was equal to 3° (——) or to −3° (—). The parameters of the model circuit corresponded to those characteristic for Sf9 cells and erythrocytes. G_p was increased linearly from 1 to 100 nS.

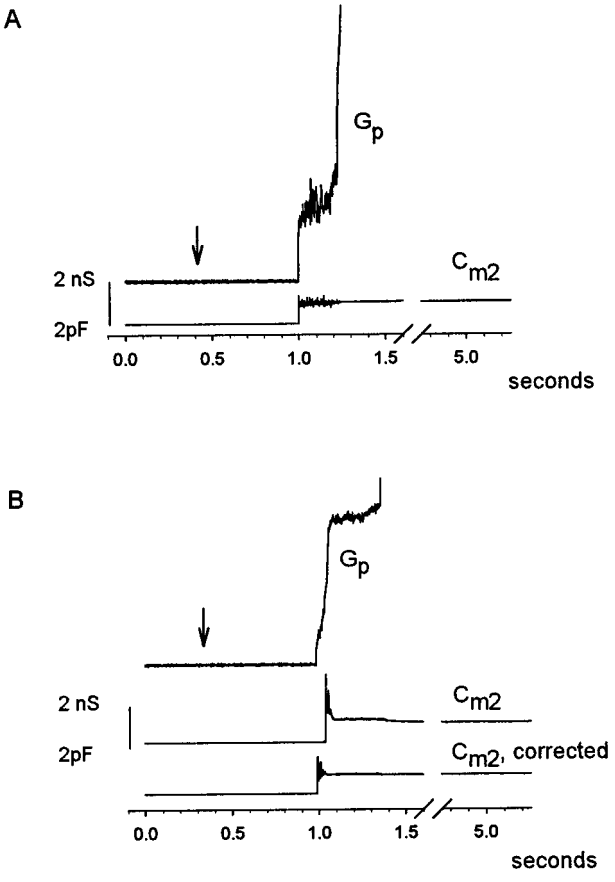

FIGURE 3 Off-line phase correction. Experiments on insect cell-erythrocyte fusion are used to demonstrate phase-related errors in the computation of membrane parameters. Here G_p and C_{m2} are calculated on the basis of the in-phase and out-of-phase software signals as described in Materials and Methods. (*A*) Fusion induces a steplike increment of the C_{m2} trace, indicating that in this experiment, phase was adjusted correctly. Background noise in the G_p trace is simply that of the in-phase software channel; before fusion occurred, C_{m2} was defined as zero. Here and in *B*, the arrow shows the onset of a pressure pulse delivering acid solution to the cell surface. (*B*) The characteristic overshoot in C_{m2} (*middle trace*) indicates that at the moment when fusion has occurred, the phase deviated from its desired value. Off-line addition of 5° to the experimental phase value improves the shape of C_{m2} (*bottom trace*), but does not affect G_p (not shown). The adjustment of the C_{m2} shape can be used to adjust the phase off-line.

A more confusing situation arises when the phase is "undercompensated" ($\varphi + 2\phi < 0$; see Eq. 24). In Fig. 3 *B*, the C_{m2} trace lags fusion simply because the fusion-induced increment of the out-of-phase signal is less than the software detection limit (defined as the point that exceeds twice the standard deviation of the preceding base line). As soon as the out-of-phase signal was detected, the calculated value of C_{m2} exceeded 1 pF. As predicted, this error vanished with the widening of the fusion pore. Adding +5° to the known experimental phase (in the off-line analysis of the data) recovered much of the natural shape of this capacitance increment, and the lag between the G_p and C_{m2} traces vanished. The adjustment of the shape of the C_{m2} trace can be used for the final correction of the phase setting long after an experiment has been finished.

DISCUSSION

Studies on membrane fusion are conducted using a wide variety of modern methods, including biochemistry, molecular biology, and x-ray crystallography. Compared to other functional assays, electrophysiological methods provide faster time resolution (up to hundreds of microseconds) and higher amplitude resolution (the fusion of a single submicron intracellular vesicle with the plasma membrane (Lollike et al., 1995). Changes in capacitance monitor fusion: it is the conductance and kinetics of formation and widening

of the fusion pore that contain information about its immediate mechanisms.

The calculation of membrane parameters starts with an accurate measurement of the source (cell and pipette) admittance. The source admittance, before entering a PSD, is distorted by low-pass filtering due to different pieces of electrophysiological equipment. Some of the approaches of the Lindau-Neher type are sensitive to this phase offset-induced distortion (i.e., they do not have built-in phase adjustment procedures). A few methods of resolving this problem have been proposed. Analog phase shifters are used by Rohlicek and Schmid (1994) to null out the phase offset. Gillis (1995) describes an empirical procedure, suggesting the insertion of a capacitor or a resistor into the input of an amplifier and a subsequent compensatory tuning of the lock-in phase angle. The phase found by this technique is affected by the signal frequency, analog filter settings, and sampling rate, and therefore it should be redefined quite often. Donnelly (1994) suggested the following procedure: 1) an outside source generates a signal with known amplitude and phase with respect to a stimulus sine wave; 2) this signal is applied to the equipment (filter) and 3) is acquired for subsequent calculation of the filter compensation vector, which 4) is subsequently used to correct experimental signals. We propose the use of the patch-clamp amplifier compensation circuitry as a source for such a signal. A displacement of a C-slow potentiometer simulates changes in the source admittance. Such changes, recorded by the phase-sensitive software, are compared to its theoretically expected amplitude. The phase is then calculated based on the divergence of these two values, which is caused by the equipment-related phase offset. Our new procedure for determination of phase distortion can be built into LN or MSW. This method of cell-pipette admittance reconstruction does not require the additional hardware suggested by Donnelly (1994) or Rohlicek and Schmid (1994), nor does it need readjustments, characteristic of the empirical procedure, proposed by Gillis (1995).

The LN approach imposes strict requirements on the membrane resting potential. For proper implementation, it requires E_r to be equal to zero or to be known and constant, a condition that may not occur in practice, because of changes in the ionic composition of a cell during an experiment. MSW solves this problem: one can calculate R_a, C_{m1}, and G_{m1}, ignoring E_r. However, if stimulating sine waves are superimposed on the holding potential, E_r can easily be calculated, which may aid in the simultaneous recording of changes in cell conductance and capacitance.

Unlike LN, PL has a built-in phase adjustment procedure that requires dithering of two potentiometers: C-slow and the one in the PSD phase circuitry. Our own experience shows that a graceful performance of this procedure requires some practice. Fortunately, the NM technique of the phase adjustment can easily be automated. A displacement of a C-slow potentiometer can be used to calculate the argument of the corresponding signal. If the argument deviates from $3\pi/2$, the software phase is adjusted to correct this deviation. Thus calibration (finding $|T(\omega)|^2$) and phase setting can be combined in a software implementation of PL.

Compared to PL, the advantage of MSW is the calculation of all three parameters of the first membrane. Although MSW in its initial form does not consider the fusion pore, we show how knowledge of R_a, C_{m1}, G_{m1} and the phase can be used to restore values of all three elements of the second (fusing) membrane. Indeed, if all elements of the first cell are known, the admittance of the fusing circuitry Y_2 can be restored, and subsequent calculation of G_p, G_{m2}, and C_{m2} can be performed under conditions that are not as strict as the ones imposed by other PL-based methods (Breckenridge and Almers, 1987; Lindau, 1991). Our modification of MSW requires only the constancy of R_a, C_{m1} during fusion. Any PL-based method suggests an accurate and long-lasting compensation of first cell parameters (i.e., $G_{sr} \cong 1/R_a$ and $C_{sl} \cong C_{m1}$). Furthermore, G_{m2}, the element neglected by other methods, can be calculated by our algorithm.

Finally, if all attempts to find the correct phase have failed and φ at the very moment of fusion deviated from the desirable angle, this deviation can be detected off-line by examination of the capacitance trace shape. Theoretically, the fusion-induced increment of the capacitance trace should look like a step function. However, if C_{m2} is calculated using only the out-of-phase PSD signal, the C_{m2} trace rises gradually, indicating the development of a fusion pore. Obviously, a command potential drops across G_p, C_{m2} in series in such a way that if the pore is narrow, a resulting current partially escapes the out-of-phase signal and shows up in the in-phase signal. Lindau (1991) introduced an algorithm of capacitance shape restoration that uses both PSD signals for the calculation of C_{m2}. If this algorithm has been applied, and C_{m2} still does not look "perfect," a deviation of the phase from its desired value can be suspected. Off-line adjustment of the phase can restore the steplike increment of C_{m2} required by membrane fusion. The opposite is also true: such restoration can be a good indicator of a successful phase angle correction. The off-line phase setting procedure suggested here has more than just a cosmetic value. Although pore conductance calculations show a relative insensitivity to the phase offset when G_p is small, this error increases with pore widening. Thus off-line phase tuning can be included in the methodological repertoire of those researchers who are interested in exploring the dynamics of pore widening and the forces governing pore enlargement.

The modified MSW and the off-line phase setting presented here could be of special importance for those studying virus-induced cell-cell fusion, where pores can be "frozen" in their low conductive states for a long period of time, and the specific resistance of the second membrane could be higher than that of a small exocytotic granule.

We are grateful to Dr. G. Blissard for providing us with an insect cell line; A. Pomerantz, ALA Scientific Instruments, for technical consultations; Dr.

Chernomordik and E. Leikina for sharing their findings regarding GP64-induced Sf9/RBC fusion; E. Leikina for preparation of erythrocytes; and O. Plonskaia for help with the manuscript.

REFERENCES

Barnett, D. W., and S. Misler. 1997. An optimized approach to membrane capacitance estimation using dual-frequency excitation. *Biophys. J.* 72: 1641–1658.

Breckenridge, L. J., and W. Almers. 1987. Currents through the fusion pore that forms during exocytosis of a secretory vesicle. *Nature.* 328: 814–817.

Curran, M., F. S. Cohen, D. E. Chandler, P. J. Munson, and J. Zimmerberg. 1993. Exocytotic fusion pores exhibit semi-stable states. *J. Membr. Biol.* 133:61–75.

Donnelly, D. F. 1994. A novel method for rapid measurement of membrane resistance, capacitance and access resistance. *Biophys. J.* 66:873–877.

Gillis, K. 1995. Techniques for membrane capacitance measurements. *In* Single-Channel Recording, 2nd Ed. B. Sakmann and E. Neher, editors. Plenum Press, New York.

Joshi, C., and J. M. Fernandez. 1988. Capacitance measurements: an analysis of the phase detector technique used to study exocytosis and endocytosis. *Biophys. J.* 53:885–892.

Lanzrein, M., N. Kasermann, R. Weingart, and C. Kempf. 1993. Early events of Semliki forest virus-induced cell-cell fusion. *Virology.* 196: 541–547.

Lindau, M. 1991. Time resolved capacitance measurements: monitoring exocytosis in single cells. *Q. Rev. Biophys.* 24:75–101.

Lindau, M., and E. Neher. 1988. Patch-clamp techniques for time resolved capacitance measurements in single cells. *Pflugers Arch.* 411:137–146.

Lollike, K., N. Borregaard, and M. Lindau. 1995. The exocytotic fusion pore of small granules has a conductance similar to an ionic channel. *J. Cell Biol.* 129:99–104.

Neher, E., and A. Marty. 1982. Discrete changes of cell membrane capacitance observed under conditions of enhanced secretion in bovine adrenal cromaffin cells. *Proc. Natl. Acad. Sci. USA.* 79:6712–6716.

Plonsky, I., and J. Zimmerberg. 1996. The initial fusion pore induced by baculovirus GP64 is large and forms quickly. *J. Cell Biol.* 135: 1831–1839.

Rohlicek, V., and J. Rohlicek. 1993. Measurement of membrane capacitance and resistance of single cells using two frequencies. *Physiol. Res.* 42:423–428.

Rohlicek, V., and A. Schmid. 1994. Dual-frequency method for synchronous measurement of cell capacitance, membrane conductance and access resistance on single cells. *Pflugers Arch.* 428:30–38.

Spruce, A. E., A. Iwata, J. M. White, and W. Almers. 1989. Patch clamp studies of single cell-fusion events mediated by a viral protein. *Nature.* 342:555–558.

Zimmerberg, J. 1993. Simultaneous electrical and optical measurements of individual membrane fusion events during exocytosis. *Methods Enzymol.* 221:99–112.

Zimmerberg, J., R. Blumenthal, D. P. Sarkar, M. Curran, and S. J. Morris. 1994. Restricted movement of lipid and aqueous dyes through pores formed by influenza hemagglutinin during cell fusion. *J. Cell Biol.* 127:1885–1894.

Zimmerberg, J., M. Curran, F. S. Cohen, and M. Brodwick. 1987. Simultaneous electrical and optical measurements show that membrane fusion precedes secretory granule swelling during exocytosis of beige mouse mast cells. *Proc. Natl. Acad. Sci. USA.* 84:1585–1589.